# On the vertical profile of stratus liquid water flux using a millimeter cloud radar


Shelby Frisch — Colorado State University

Paquita Zuidema — University of Colorado

Chris Fairall — NOAA

Environmental Technology Laboratory, Boulder, CO


## 1. Introduction

Millimeter cloud radars are routinely applied towards estimating liquid water contents and droplet sizes within all-liquid, non-drizzling stratus clouds. By including additional information about droplet fall velocities, a liquid water flux due to the mean fall velocity of the cloud droplets can also be estimated for non-drizzling stratus. Previous work has shown this can be comparable to the turbulent liquid water flux (Nicholls, 1984). Nicholls (1984) also found that calculations of the implied cloud-top entrainment were sensitive to the liquid water flux term, because the liquid water flux offsets the apparent upward moisture flux. Given the importance of the liquid water flux towards the total liquid water budget, the associated latent heating may potentially contribute significantly to the total diabatic heating.

In this poster we estimate the liquid water flux from cloud radar reflectivities and an independently-derived cloud number concentration for two days of non-drizzling stratus. Through assuming horizontal homogeneity, the time rate of change of the liquid water flux is the vertical gradient of the liquid water flux. The latent heating is estimated and compared to the total radiative heating, towards assessing its importance.

The NOAA Research Vessel Ronald H. Brown (RHB) participated in a two-week stratocumulus study in the southeastern Pacific during October, 2001, as part of the East Pacific Investigation of Climate Processes (EPIC-2001). Its goals included an increased understanding of the heat and water fluxes for this region, and the measurement of the vertical structure of the atmospheric boundary layer. A cloud radar (Ka-band, 8.66 mm wavelength) was present on the RHB during this time.

We focus upon two days of stratus observed on Oct. 23-24, 2001 at approximately 20S and 75 W, off of the northern coast of Chile.

## 2. Method

The liquid water flux due to the cloud droplet fall velocity can be written as

$$\overline{q_l w_t} = \frac{4\pi}{3} N \rho_l \int_0^\infty r^3 w_t(r) f(r) dr \qquad (1)$$

where $q_l w_t$ is the liquid water flux, $r$ is the droplet radius, $f(r)$ is the droplet distribution, $N$ is the droplet concentration, and $\rho_l$ is the density of the liquid. For non-drizzling cloud droplets, we can assume that the fall velocity $w_t$ will be in the Stokes range, or $w < 0.4$ m/s. Beard and Pruppacher (1969) show that the terminal velocity of a sphere for Stokes flow is

$$w_t(r) = \frac{2}{9}[g(\rho_l - \rho_a)\eta]r^2 \qquad (2)$$

where $g$ is the acceleration due to gravity, $\eta$ is the vicosity of air, and $\rho_a$ is the density of air. Substituting (2) into (1), and noting that we have

$$\overline{q_l w_t} = \frac{8\pi}{27\eta} N \rho_l^2 g < r^5 > \qquad (3)$$

For a log-normal droplet distribution, the moments of $r$ become

$$< r^k > = r_o^k exp(k^2 \sigma_x^2/2) \qquad (4)$$

(Frisch et al., 1995) where $r_o$ is the logarithmic mean droplet radius and $\sigma_x$ is the logarithmic spread of the droplet distribution. Using (3), the vertical liquid water flux becomes

$$\overline{q_l w_t} = \frac{8\pi}{27\eta} N \rho_l^2 g r_o^5 exp(25\sigma_x^2/2) \qquad (5)$$

Frisch et al. (2002) show that the effective radius of log-normally distributed stratus cloud droplets relate to the radar reflectivity $Z$ through

$$r_e = \frac{1}{2}\left(\frac{Z}{N}\right)^{\frac{1}{6}} exp(-0.5\sigma_x^2) \qquad (6)$$

where $r_e$ is the effective radius and is related to the median radius through

$$r_e = \frac{< r^3 >}{< r^2 >} \qquad (7)$$

Combining (4) through (7) gives

$$\overline{q_l w_t} = \frac{\pi}{128\eta} N^{\frac{1}{6}} \rho_l^2 g Z^{\frac{5}{6}} exp(-2.5\sigma_x^2) \qquad (8)$$

The liquid water flux as a function of the radar reflectivity is shown graphically below.

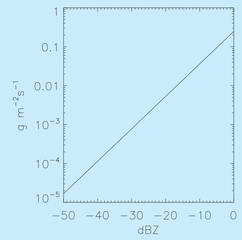


We estimate an error in the liquid water flux of approximately 40 % due to variability in N and the logarithmic width . This is based on a mean number concentration of 98 /cc with a standard deviation of 78 /cc, and a mean logarithmic width of 0.32 with a standard deviation of 0.09, from *in situ* observations made during the Surface Heat Budget of the Arctic experiment and the Atlantic Stratocumulus Experiment . The Stokes range assumption requires non-drizzling conditions, established here using a reflectivity threshold of -17 dBZ. This corresponds to a liquid water flux of 0.02 g/(m*m s).

The associated latent heating, assuming horizontally homogeneous conditions, is then estimated as

$$\frac{\partial T}{\partial t} = -\frac{L}{\rho_a c_p} \frac{\partial \overline{q_l w_t}}{\partial z} \qquad (9)$$

where $T$ is the temperature, $L$ is the latent heat of vaporization, and $c_p$ is the heat capacity of air at constant pressure. In practice, a centered finite difference calculation is done, so that the estimated latent heating error is 45%.

## 3. The example case

October 23-24 were near the end of the stratocumulus study, with the research vessel moving back towards the Chilean coast. No drizzle was observed on the surface on either day, and a cloud droplet concentration of approximately 400 /cc was inferred from solar transmission measurements. This value was high compared to other days and can help explain the lack of drizzle.

The top panel of the figure below shows the cloud radar reflectivities for both days and includes the surface-based ceilometer-derived cloud base.

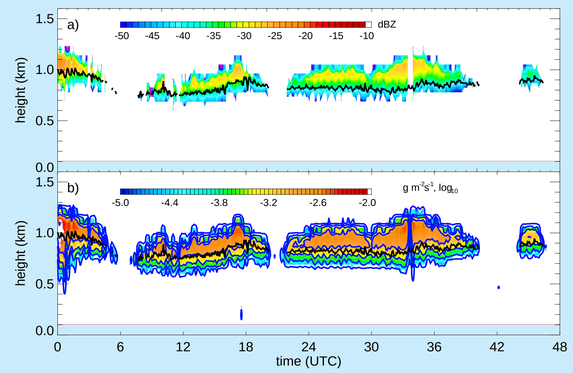


Fig. 1 a) cloud radar reflectivities for Oct. 23-24, 2001. b) the associated liquid water flux, calculated using N=400 /cc and a logarithmic droplet distribtuion width of 0.35. Liquid water contours are shown for values of 0.01 and 0.1 g/(m^3).

The bottom panel shows the liquid water flux corresponding to the gravitation settling of the non-drizzling cloud drops. The maximum value is approximately 0.005 g/(m*m*s). Relative maxima occur within the upper half of the cloud

## 4. Latent Heating and Radiative Heating Field

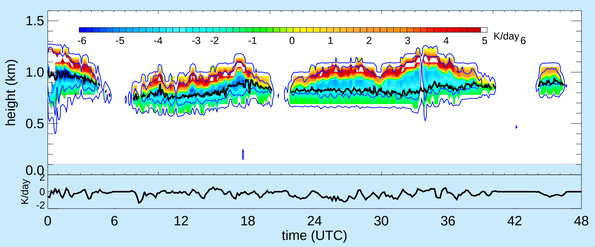


Fig. 2: The latent heating associated with the liquid water fluxes shown in Fig. 1, using Eqn. (11) (top panel). Liquid water contours are shown at 0.01 and 0.1 g/(m^3) and the ceilometer-sensed cloud base is also shown. The bottom panel shows the vertically-integrated latent heating

Fig. 2 shows the estimated latent heating field. The latent heating ranges between -4 to +6 K/day, with condensational heating evident within the upper-half of the cloud, and evaporative cooling in the lower-half of the cloud. The vertically-integrated latent heating rate is often near zero, consistent with a total water content (water vapor + liquid) remaining constant with height.

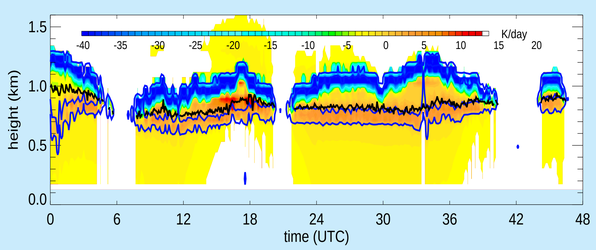


Fig. 3: The net radiative heating, calculated as longwave+shortwave - (clear sky longwave+shortwave) (top panel). Liquid water contours are shown at 0.01 and 0.1 g/(m^3) and the ceilometer-sensed cloud base is also shown.

Fig. 3 shows the net broadband radiative heating rates, to help assess the relative importance of the latent heating. The radiative heating rates were calculated using the radiative transfer model Streamer. and use temperature and relative humidities interpolated from the available soundings. Solar noon occurs at approximately 17 and 41 UTC and is evident as lessened cloud-top cooling and enhanced within-cloud warming.

## 5. Discussion

During two days of non-drizzling stratus observed off of the northern Chilean coast, an estimated liquid water flux ranged up to 0.005 g m$^{-2}$ s$^{-1}$, corresponding to latent heatings between +6 K/day to -4 K/day. Compared to cloud-top radiative cooling rates of -40 K/day, and maximum radiative heating rates approaching 15 K/day within the cloud at solar noon, the latent heating associated with the gravitational settling of the cloud drops is typically approximately 10%. This is small but not negligible.

The radiative and latent heating terms are generally opposite in sign, so that near cloud-top, neglect of latent heating from droplet gravitational settling would lead to an overestimate of the total diabatic heating. Lower down within the cloud, the two terms are more balanced, except during solar noon, when shortwave absorption dominates the evaporative cooling term.

During EPIC significant drizzle often evaporated completely below cloud base (Bretherton et al., 2003). The associated latent cooling will be more pronounced and will lead to different conclusions than those presented here. The vertical turbulent liquid water flux term has also been ignored here.


References:

Beard and Pruppacher, 1969: A determination of the terminal velocity and drag of small water drops by means of a wind tunnel. *J. Atmos. Sci.*, **26**, p. 1066-1971.

Bretherton, C.S., T. Uttal, C. Fairall, S. E. Yuter, R.A. Weller, D. Baumgardner, K. Comstock, and R. Wood, 2003: The EPIC stratocumulus study. *Bull. Amer. Meteor. Soc.*, submitted.

Frisch. A. S., C. Fairall , and J. B. Snider, 1995: Measurement of stratus cloud and drizzle parameters in ASTEX with a K-band Doppler radar and a microwave radiometer. *J. Atmos. Sci.*, **52,** 2788-2799.

Frisch, A. S., M. Shupe, I. Djalalova, G. Feingold, and M. Poellot, 2002: The retrieval of stratus cloud droplet effective radius with cloud radars. *J. Atmos. Oc., Tech.* **19**, 835-842.

Key, J. 2001: Streamer User's Guide. *Cooperative Institute for Meteorological satellite Studies,* 96 pp.

Nicholls, S., 1984: The dynamics of stratocumulus: aircraft observations and comparisons with a mixed-layer model. *Quart. J. Roy. Meteor. Soc.*, **110,**783-820.